Electrochemistry Communications 154 (2023) 107544

Contents lists available at ScienceDirect

Electrochemistry Communications

journal homepage: www.elsevier.com/locate/elecom

Full Communication

Formation of an organic film on an electrode via a suspension of redox-active droplets in acidic aqueous solution

Katarzyna Dusilo [a], Aleksandra Siwiec [a], Marcin Holdynski [a], Pekka Peljo [b], Marcin Opallo [a,*]

[a] Institute of Physical Chemistry, Polish Academy of Sciences, Warszawa, Poland
[b] Research Group of Battery Materials and Technologies, Department of Mechanical and Materials Engineering, University of Turku, Turku, Finland

ARTICLE INFO

Keywords:
Emulsion
Redox reaction
Ionic liquid
Decamethylferrocene
Toluene

ABSTRACT

Previous electrochemical studies of redox emulsions have been mainly performed in the context of electro-organic synthesis. More recently, this research has been oriented towards applications of emulsions in flow batteries. Such biphasic systems seem to provide a suitable environment for reactions at the liquid–liquid interface. Taking an emulsion consisting of microdroplets of decamethylferrocene solution in a hydrophobic ionic liquid/toluene mixture in acidic aqueous solution as an example, we have demonstrated that an electrochemical redox reaction involving the hydrophobic redox probe occurs at the glassy carbon electrode|organic liquid film interface. This reaction is followed by ion exchange between liquid phases. This effect is explained by the instability of the emulsion. A portion of the organic liquid stays on the electrode surface after transfer to a purely aqueous electrolyte and remains electroactive.

1. Introduction

More than 40 years ago, it was demonstrated that voltammetric signals related to the electrochemical processes of organic compounds poorly soluble in water could be obtained in a micellar solution or emulsion [1]. This indicates that organic droplets approach sufficiently close to the electrode surface to allow for efficient electron transfer between molecules dissolved in the organic phase and the electrode. More recently, suspensions of droplets containing water insoluble organic reactants/catalysts have been studied in the context of electro-organic synthesis [2,3]. Currently, research on redox-active microemulsions is driven by their potential application in flow batteries [4–7].

Initially, electrochemical studies of redox-active compounds dissolved in suspended organic droplets were focused on the determination of the solute diffusion coefficient [8], the distribution of the solute between organic and aqueous phases [9] or estimation of the difference between the diffusion coefficient of the neutral redox probe and its parent cation in different phases [10]. The effect of the degree of emulsification on the electrochemistry of redox-active compounds was also studied [11]. The apparent irreversibility of the electrooxidation of ferrocene (Fc) in water–organic emulsions due to the interfacial transfer of the resulting ferrocenium cation [12], and the electrochemical coalescence of organic droplets caused by electrochemical redox reactions [13] have also been reported. It has recently been shown that the ratio between aqueous, surfactant and organic components of a microemulsion, as well the type and concentration of electrolyte, can affect the redox potential of the Fc/Fc^+ redox couple [14–16]. This was interpreted as a result of the distribution of neutral molecules and newly formed cations between organic and aqueous components. A correlation between the structure of the microemulsion and the electrochemical behaviour of ferrocene was found [17]. The effect of the gradient of the organic component in the vicinity of the electrode has been included in simulations of voltammograms and also measured experimentally [18]. Other studies of redox-active microemulsions have focused on single electrochemical events related to droplet collisions with an ultramicroelectrode [19–21].

In most of the studies mentioned above [4,5,12,14–18], ferrocene and its more hydrophobic derivatives were dissolved in the organic component of redox-active microemulsions and employed as a redox probe. The electrochemically generated cation may be transferred to the aqueous phase [12,22]; this phenomenon is less likely for more hydrophobic redox probes [22]. Therefore, decamethylferrocene (DMFc) was employed in this study. The selection of this easily oxidised hydrophobic ferrocene derivative was also driven by its applicability as an electron donor in biphasic oxygen reduction or hydrogen evolution reactions [23–26]. For the same reason, an acidic aqueous solution was employed

* Corresponding author.
E-mail address: mopallo@ichf.edu.pl (M. Opallo).

https://doi.org/10.1016/j.elecom.2023.107544
Received 28 June 2023; Received in revised form 17 July 2023; Accepted 19 July 2023
Available online 20 July 2023

as the aqueous phase. A hydrophobic ionic liquid [27] solution in toluene (TN) was selected as the organic component on the basis of earlier studies of redox emulsions [19,21,28].

2. Materials and methods

2.1. Materials

$HClO_4$ (ACS reagent, 70%) and TN (Supelco, for analysis) were supplied by Sigma Aldrich, trihexyltetradecylphosphonium bis(trifluoromethylsulfonyl)imide ($P_{(6,6,6,14)}N(Tf)_2$) (Fig. S1) (>98 %) was purchased from Iolitec. DMFc (97 %) and KPF_6 (99 %) were obtained from Aldrich Chemistry, $NaClO_4$ (≥98 %) from Fluka Analytical, NaSCN (≥98.0 %) from Fluka Chemica and KNO_3 (pure for analysis) from Chempur.

The Arium® Comfort Lab Water System (Sartorius) was used to prepare deionized water with a resistivity of 18.2 MΩ·cm for the aqueous solutions.

2.2. Methods

An emulsion was prepared using 0.1 ml of 5 mM DMFc solution in 400 mM $P_{(6,6,6,14)}N(Tf)_2$ solution in TN (later called $P_{(6,6,6,14)}N(Tf)_2$/TN) and 5 ml of 0.1 M $HClO_4$ solution. The liquids were mixed using a vortex VELP Scientifica F202A0175 for 20 s. The mixture was then ultrasonicated in a bath using an EMAG Emmi-30HC for 3 s at full power and then turned off for 7 s [19]. This was repeated 20 times, after which a cloudy appearance was seen (Fig. S2). After 2–3 h the first droplets of the organic phase were visible to the naked eye. Dynamic light scattering experiments (DLS Zetasizer) did not give reproducible results, but the zeta potential value was around −10 mV, indicating emulsion instability.

Electrochemical experiments (cyclic voltammetry, chronoamperometry, square wave voltammetry (SWV)) were performed with an Autolab PGSTAT30 potentiostat, in a three-electrode system using a glassy carbon electrode (3 mm diameter) as the working electrode, Ag|AgCl|NaCl 3 M or silver wire as the reference, and platinum wire as the counter electrode. Some measurements were carried out with a platinum ultramicroelectrode (UME) of diameter 60 μm. All electrochemical experiments were performed at room temperature and most of them in solutions stirred by an IKA magnetic stirrer.

Scanning electron microscope (SEM) images and EDS results were obtained using a FEI Nova NanoSEM 450 equipped with an EDS detector.

3. Results and discussion

The peak-shaped voltammograms recorded in a stirred redox-active emulsion (Fig. 1) indicate that the efficiency of the diffusion-controlled simple reversible oxidation–reduction process:

$$DMFc(org) - e^- \leftrightarrow DMFc^+(org) \quad (1)$$

is not affected by convective transport of the redox-active droplets. When the organic phase is in contact with an aqueous electrolyte, reaction (1) is followed by ion exchange between $P_{(6,6,6,14)}N(Tf)_2$/TN and the aqueous electrolyte in order to maintain electroneutrality [29–31] (see below).

Reaction (1) is controlled by diffusion, as confirmed by the linear dependence of the peak current on the square root of the scan rate, which is observed for both stirred and non-stirred solutions (see Fig. 1 insert). The minor influence of the stirring rate on the magnitude of the peak current implies that the electrode process is only slightly affected by forced convection. The difference between peak potentials is much larger than expected for pure diffusional control and is probably caused by an uncompensated ohmic drop (Figs. 1, S3, S4, S5).

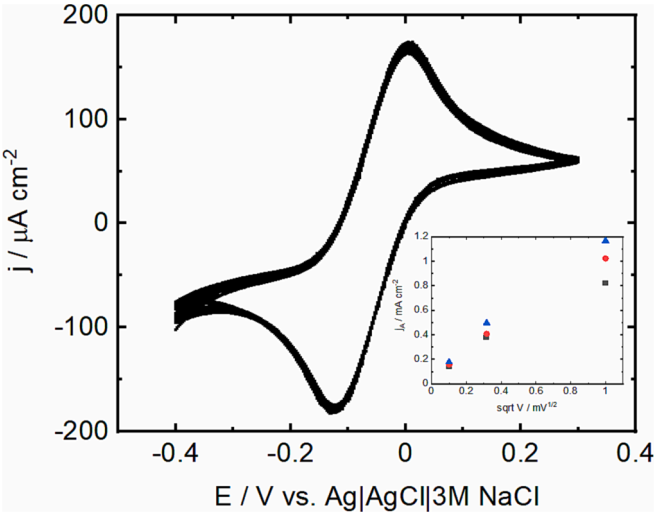

Fig. 1. Consecutive cyclic voltammograms (90 cycles) recorded at a GC electrode in a stirred emulsion (200 rpm) consisting of 100 μl of 5 mM DMFc and 400 mM $P_{(6,6,6,14)}N(Tf)_2$ solution in toluene and 5 ml of 0.1 M $HClO_4$ aqueous solution. The scan rate was 10 mV s^{-1}. The insert shows the anodic current dependence on the square root of the scan rate in the same emulsion: not stirred (black squares), stirred at 200 rpm (red circles) and stirred at 1000 rpm (blue triangles). Data from Figs. S3, S4 and S5.

The positions of the voltammograms obtained with an ultramicroelectrode in DMFc solution in $P_{(6,6,6,14)}N(Tf)_2$/TN with respect to the current axis (Fig. S6) indicates that almost half of the DMFc molecules have been oxidised by oxygen dissolved in the solution. As this reaction requires protons [23], some moisture must be present in the aqueous phase and/or some acid must be present in the ionic liquid. This reaction can also be catalysed by an ionic liquid cation, as previously observed for alkali metal cations [32,33]. In turn, the peak currents of voltammograms recorded with a GC disc electrode in five-times diluted DMFc solution in $P_{(6,6,6,14)}N(Tf)_2$/TN (Fig. S7), are close to half of that obtained in an experiment performed in emulsion with the same electrode (Fig. 1). This is rather unexpected in terms of the collective effect of direct collisions of the redox-active droplets with the electrode surface, because DMFc solution in $P_{(6,6,6,14)}N(Tf)_2$/TN is a minor component of the biphasic electrolyte (0.0197 by volume). Consequently, the effective DMFc concentration in the emulsion is equal to 0.098 mM, i.e., 50 times smaller than in the bulk organic phase. Bearing in mind that the estimated viscosity of $P_{(6,6,6,14)}N(Tf)_2$/TN is close to that of water (see SI, section S5), one would expect a significantly smaller peak current in the emulsion. However, if an organic liquid film is present on the electrode surface such a peak current could be reasonable, because it is close to the value obtained in the bulk $P_{(6,6,6,14)}N(Tf)_2$/TN phase (Fig. S7). The fact that the peak current is independent of the number of scans (Fig. 1) suggests that a $P_{(6,6,6,14)}N(Tf)_2$/TN film is formed on the electrode within a minute after immersion of the GC electrode in the redox emulsion.

Formation of a DMFc-containing liquid film is confirmed by a chronoamperometric experiment in the stirred solution. When the potential of a GC electrode immersed in the redox emulsion is increased from −0.4 V to 0.5 V, the slope of the current vs. time graph (on a logarithmic scale) is close to −0.5, as expected for semi-infinite diffusion (Fig. 2A). After about 100 s the slope decreases, indicating a DMFc concentration gradient. This can be attributed to exhaustive electrolysis of the redox probe. At longer times this may result from a concentration gradient of organic droplets beyond the liquid–liquid interface [11]. Using the estimated value of the DMFc diffusion coefficient in $P_{(6,6,6,14)}N(Tf)_2$/toluene (see SI, section S5), one may calculate the thickness of the liquid film from the random walk equation – this is found to be 100–200 μm. Interestingly, the magnitude of the peak current of a voltammogram

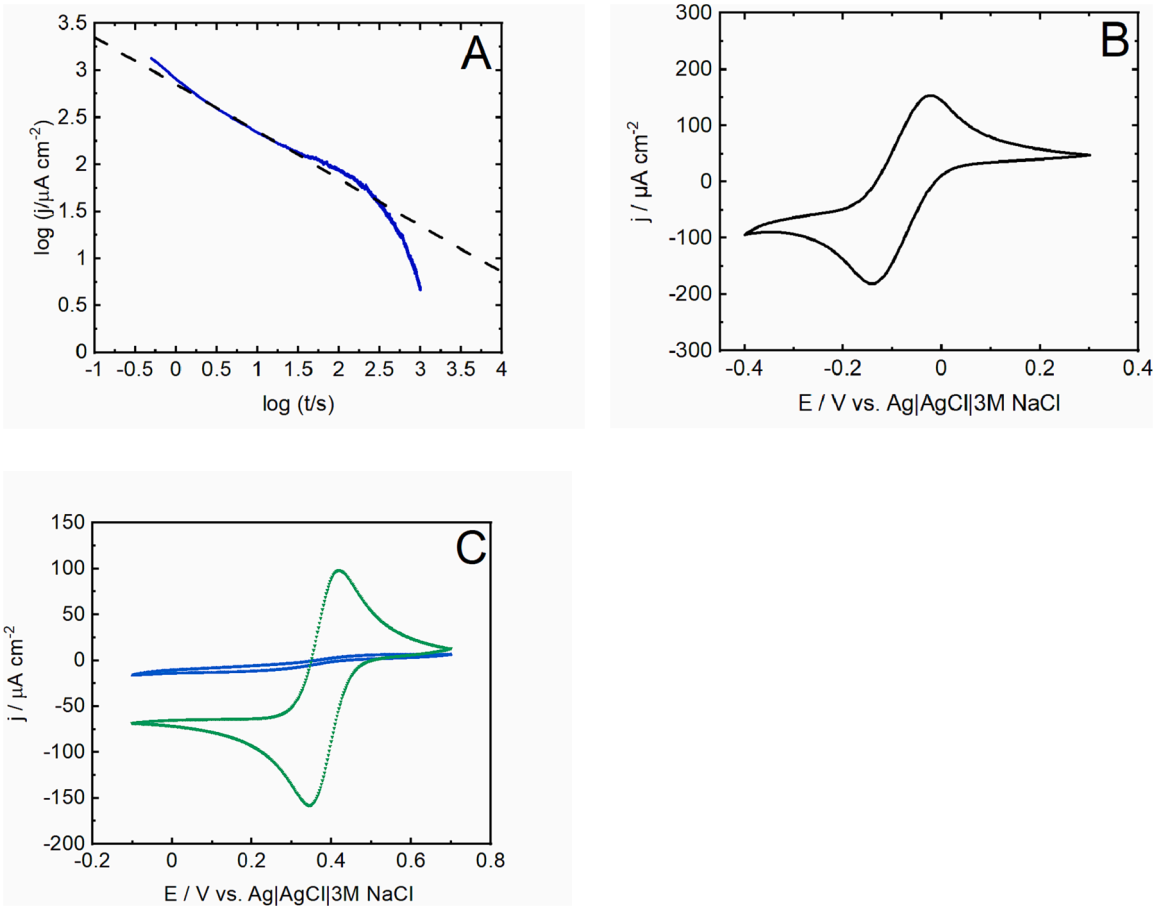

Fig. 2. (A) Chronoamperogram (blue) obtained after a potential step to 0.5 V in stirred (200 rpm) emulsion consisting of 100 μl of 5 mM DMFc 400 mM $P_{(6,6,6,14)}N(Tf)_2$ in toluene and 5 ml of 0.1 M $HClO_4$ aqueous solution. The slope of the dashed black line is −0.5. (B) Voltammogram obtained using a GC electrode modified with 8 μl of 5 mM DMFc 400 mM $P_{(6,6,6,14)}N(Tf)_2$ in toluene, immersed in 0.1 M $HClO_4$ aqueous solution. Scan rate 10 mV s^{-1}. (C) Cyclic voltammograms obtained using 2 mM $K_3[Fe(CN)_6]$ solution in 0.1 $HClO_4$ aq. in the absence (green) and presence (blue) of emulsion consisting of 100 μl of 400 mM $P_{(6,6,6,14)}N(Tf)_2$ in toluene. Scan rate 10 mV s^{-1}. (For interpretation of the references to colour in this figure legend, the reader is referred to the web version of this article.)

recorded at a GC electrode modified with 8 μl DMFc solution in $P_{(6,6,6,14)}N(Tf)_2$/TN (the volume corresponding to a 200 μm liquid film on a GC electrode) and the midpeak potential (Fig. 2B) are close to those recorded in the emulsion.

In order to further clarify the steps of reaction (1), SWV was performed with a liquid-film-modified electrode in a series of aqueous electrolytes consisting of sodium or potassium salts with PF_6^-, ClO_4^-, SCN^- and NO_3^- anions. The SWV peak potential (E_p) depends on the anion (Fig. S8). The curve of E_p dependence on the potential of anion transfer from organic to aqueous phase (Fig. S9) indicates gradual transition from anion insertion into $P_{(6,6,6,14)}N(Tf)_2$/TN to cation ejection to the aqueous phase following reaction (1) [29–31]. Therefore, one may conclude that formation of $DMFc^+$ (reaction (1)) at the solid|liquid interface is followed by further reactions at the liquid|liquid interface:

$$ClO_4^-\ (aq) \rightarrow ClO_4^-\ (org) \quad (2)$$

$$P^+_{(6,6,6,14)}(org) \rightarrow P^+_{(6,6,6,14)}(aq) \quad (3)$$

$$DMFc^+(org) \rightarrow DMFc^+(aq) \quad (4)$$

Comparison with other IL/TN systems shows that the contribution of reaction (2) vs. reactions (3) and (4) depends on the type of ionic liquid [34]. Other proof of organic liquid film formation is provided by cyclic voltammetry in a solution of the hydrophilic redox probe – $Fe(CN)_6^{3-}$ in $P_{(6,6,6,14)}N(Tf)_2$/TN emulsion. The voltammogram exhibits only traces of cathodic and anodic peaks compared to the voltammogram recorded in an aqueous solution of the same redox probe (Fig. 2C).

A so-called 'transfer experiment' demonstrates that a portion of the redox-active liquid film remains on the electrode. After a specified time (1 or 10 min) in the redox emulsion, the electrode was pulled out, washed with water and immersed in 0.1 M $HClO_4$ (aq). A series of voltammograms was then recorded (Fig. 3A). They are almost stable: a small decrease in the peak current is seen during the early scans. The peak current density is about 10 times smaller than that seen in a voltammogram obtained in contact with the emulsion, indicating that the redox active organic liquid covers only a fraction of the surface. In turn, the difference between peak potentials reduces from 0.16 to 0.03 V, pointing to restricted diffusion of the redox probe in the film [29] or solid deposit. Interestingly, this voltammogram is similar to that obtained with a carbon electrode modified with DMFc microcrystals immersed in the same electrolyte (Fig. 6 in ref. [35]). Indeed, on looking at the SEM image of the electrode after removal from the redox emulsion, microcrystals with a size in the tens of micrometers can be seen (Fig. 3B). However, they are not seen when DMFc is absent from the organic phase (Fig. S11). EDS analysis of the spots with microcrystals shows the presence of Fe (Fig. S12, S13, Table S1), which originates from DMFc crystals formed, perhaps, after evaporation of toluene from $P_{(6,6,6,14)}N(Tf)_2$/TN.

4. Conclusions

On the basis of the above results it can be concluded that an organic liquid film derived from an unstable emulsion may be formed on the

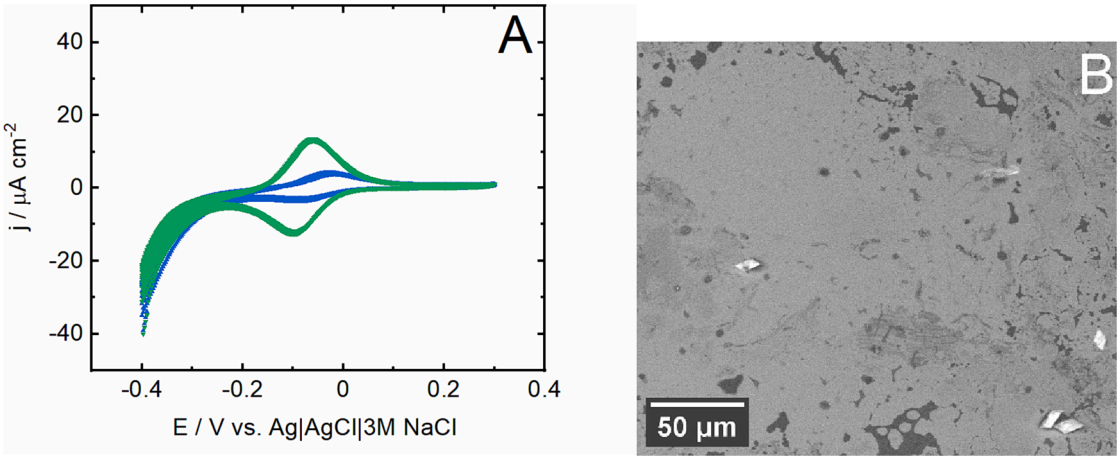

Fig. 3. (A) Cyclic voltammograms obtained at a GC electrode transferred after 1 min (blue) and after 10 min (green) from a stirred (200 rpm) emulsion consisting of 100 µl of 5 mM DMFc 400 mM $P_{(6,6,6,14)}N(Tf)_2$ in toluene and 5 ml of 0.1 M $HClO_4$ to a 0.1 M $HClO_4$ aqueous solution. No stirring, scan rate 10 mV s^{-1}, 10 scans. (B) SEM image of a GC electrode removed from the emulsion after 10 min. (For interpretation of the references to colour in this figure legend, the reader is referred to the web version of this article.)

electrode surface. As an ionic liquid is one of the components of the organic phase, formation of a liquid film may result from electrode material–ionic liquid coupling. This phenomenon has been explored for electrochemical sensing and energy storage [36–38]. In particular, deposition of droplets of a hydrophobic ionic liquid film on a GC electrode has been reported [39]. This observation may also be an extreme case of the predicted organic phase concentration gradient in the vicinity of an electrode immersed in emulsion [18]. On the other hand, it allows for a continuous supply of a redox reagent dissolved in the organic phase to the liquid film. This can also be considered as an alternative method for modifying the electrode surface with liquid, when a continuous exchange of material with suspended droplets occurs. Clearly, the suspended droplets allow for larger coverage of the electrode with a liquid film. Although the electrode material (here hydrophobic GC) may play a role, preliminary experiments with a gold electrode have led to similar observations. This approach may be useful in the analysis of redox reactions in emulsions formed by other components. It is interesting to note that the Scheludko–Exerowa thin liquid film—pressure balance technique has been applied to studies of emulsions [40].

CRediT authorship contribution statement

Katarzyna Dusilo: Investigation, Conceptualization, Data curation, Writing – review & editing. **Aleksandra Siwiec:** Investigation. **Marcin Holdynski:** Investigation, Writing – review & editing. **Pekka Peljo:** Writing – review & editing, Funding acquisition. **Marcin Opallo:** Writing – original draft, Funding acquisition, Supervision.

Declaration of Competing Interest

The authors declare that they have no known competing financial interests or personal relationships that could have appeared to influence the work reported in this paper.

Data availability

Data will be made available on request.

Acknowledgements

The help of Dr. Tomasz Andryszewski in DLS experiments is greatly appreciated.

This work was financially supported by the National Science Centre (NCN, Poland) through grant UNISONO Solar-Driven Chemistry No. 2019/01/Y/ST4/00022, and by Academy of Finland Solar-Driven Chemistry project No. 334828.

Appendix A. Supplementary data

Supplementary data to this article can be found online at https://doi.org/10.1016/j.elecom.2023.107544.

References

[1] T.C. Franklin, M. Iwunze, Oxidative voltammetry of organic compounds at platinum electrodes in micelle and emulsion systems, Anal. Chem. 52 (1980) 973–976, https://doi.org/10.1021/ac50056a045.
[2] J.D. Watkins, F. Marken, Application of ionic liquids, emulsions, sonication, and microwave assistance, in: O. Hammerich, B. Speiser (Eds.), Organic Electrochemistry, CRC Press, 2015, pp. 331–344, https://doi.org/10.1201/b19122.
[3] F. Marken, J.D. Wadhawan, Multiphase methods in organic electrosynthesis, Acc. Chem. Res. 52 (2019) 3325–3338, https://doi.org/10.1021/acs.accounts.9b00480.
[4] B.A. Barth, A. Imel, K. McKensie Nelms, G.A. Goenaga, T. Zawodzinski, Microemulsions: breakthrough electrolytes for redox flow batteries, Front. Chem. 10 (2022) 831200, 10.3389/fchem.2022.831200.
[5] X. Chen, N. Sinclair, J. Wainwright, A. Imel, B. Barth, T.A. Zawodzinski, R. F. Savinell, A study of ferrocene diffusion in toluene/Tween 20/1-butanol/water microemulsions for redox flow battery applications, J. Electrochem. Soc. 168 (2021), 060539, https://doi.org/10.1149/1945-7111/ac0b26.
[6] K. Nakao, K. Noda, H. Hashimoto, M. Nakagawa, T. Nishimi, A. Ohira, Y. Sato, D. Kato, T. Kamata, O. Niwa, M. Kunitake, Electrochemistry in bicontinuous microemulsions derived from two immiscible electrolyte solutions for a membrane-free redox flow battery, J. Coll. Interface. Sci. 641 (2023) 348–358, https://doi.org/10.1016/j.jcis.2023.03.060.
[7] Y. Zheng, A.P. Ramos, H. Wang, G. Alvarez, A. Ridruejo, J. Peng, Non-aqueous organic redox active materials for a bicontinuous microemulsion-based redox flow battery, Materials Today Energy 34 (2023), 101286, https://doi.org/10.1016/j.mtener.2023.101286.
[8] T. Matsubara, J. Texter, In situ voltammetric determinations of solute distribution coefficients in emulsions, J. Colloid Interface Sci. 112 (1986) 421–426, https://doi.org/10.1016/0021-9797(86)90110-4.
[9] J. Texter, T. Beverly, S.R. Templar, T. Matsubara, Partitioning of para-phenylenediamines in oil-in-water emulsions, J. Colloid Interface Sci. 120 (1987) 389–403, https://doi.org/10.1016/0021-9797(87)90366-3.
[10] J. Georges, S. Desmettre, Electrochemical oxidation of hydrophobic compounds in aqueous micellar solutions and oil-in-water emulsions, Electrochim. Acta 31 (1986) 1519–1524, https://doi.org/10.1016/0013-4686(86)87070-0.
[11] F. Marken, R.G. Compton, Sonoelectrochemically modified electrodes: ultrasound assisted electrode cleaning, conditioning, and product trapping in 1-octanol/water emulsion systems, Electrochim. Acta 43 (1998) 2157–2165, https://doi.org/10.1016/S0013-4686(97)10008-1.
[12] J. Chen, O. Ikeda, K. Aoki, Electrode reaction of ferrocene in a nitrobenzene + water emulsion, J. Electroanal. Chem. 496 (2001) 88–94, https://doi.org/10.1016/S0022-0728(00)00240-0.

[13] Y. Yoshida, J. Chen, K. Aoki, Electrochemical coalescence of nitrobenzene | water emulsions, J. Electroanal. Chem. 553 (2003) 117–124, https://doi.org/10.1016/S0022-0728(03)00304-8.
[14] J. Peng, N.M. Cantillo, K. McKensie Nelms, L.S. Roberts, G. Goenaga, A. Imel, B. A. Barth, M. Dadmun, L. Heroux, D.G. Hayes, T. Zawodzinski, Electron transfer in microemulsion-based electrolytes, ACS Appl, Mater. Interfaces 12 (2020) 40213–40219, https://doi.org/10.1021/acsami.0c07028.
[15] J. Peng, Y. Xao, A. Imel, B.A. Barth, N.M. Cantillo, K. McKensie Nelms, T. A. Zawodzinski, Electrolyte effects on the electrochemical performance of microemulsions, Electrochim. Acta 393 (2021), 139048, https://doi.org/10.1016/j.electacta.2021.139048.
[16] A.P. Ramos, Y. Zheng, J. Peng, A. Ridruejo, Structure, partitioning, and transport behavior of microemulsion electrolytes: molecular dynamics and electrochemical study, J. Mol. Liq. 380 (2023), 121779, https://doi.org/10.1016/j.molliq.2023.121779.
[17] A.E. Imel, B. Barth, D.G. Hayes, M. Dadmun, T. Zawodzinski, Microemulsions as emerging electrolytes: the correlation of structure to electrochemical response, ACS Appl. Mater. Interfaces 14 (2022) 20179–20189, https://doi.org/10.1021/acsami.2c00181.
[18] T. Tichter, R. Borah, T. Nann, A theoretical framework for the electrochemical characterization of anisotropic micro-emulsions, ChemElectroChem 8 (2021) 3397–3409, https://doi.org/10.1002/celc.202100600.
[19] B.K. Kim, A. Boika, J. Kim, J.E. Dick, A.J. Bard, Characterizing emulsions by observation of single droplet collisions—attoliter electrochemical reactors, J. Am. Chem. Soc. 136 (2014) 4849–4852, https://doi.org/10.1021/ja500713w.
[20] W. Cheng, R.G. Compton, Oxygen reduction mediated by single nanodroplets containing attomoles of vitamin B12: electrocatalytic nano-impacts method, Angew. Chem. Int. Ed. 54 (2015) 7082–7085, https://doi.org/10.1002/anie.201501820.
[21] C. Liu, P. Peljo, X. Huang, W. Cheng, L. Wang, H. Deng, Single organic droplet collision voltammogram via electron transfer coupled ion transfer, Anal. Chem. 89 (2017) 9284–9291, https://doi.org/10.1021/acs.analchem.7b02072.
[22] G. Shul, M. Opallo, Ion transfer across liquid–liquid interface coupled to electrochemical redox reaction at carbon paste electrode, Electrochem. Commun. 7 (2005) 194–198, https://doi.org/10.1016/j.elecom.2004.12.008.
[23] B. Su, R. Partovi-Nia, F. Li, M. Hojeij, M. Prudent, C. Corminboeuf, Z. Samec, H. Girault, H_2O_2 generation by decamethylferrocene at a liquid|liquid interface, Angew. Chem. Int. Ed. 47 (2008) 4675–4678, https://doi.org/10.1002/ange.200801004.
[24] I. Hatay, B. Su, F. Li, R. Partovi-Nia, H. Vrubel, X. Hu, M. Ersoz, H.H. Girault, Hydrogen evolution at liquid–liquid interfaces, Angew. Chem. Int. Ed. 48 (2009) 5139–5142, https://doi.org/10.1002/ange.200901757.
[25] M. Opallo, K. Dusilo, M. Warczak, J. Kalisz, Hydrogen evolution, oxygen evolution, and oxygen reduction at polarizable liquid|liquid interfaces, ChemElectroChem 9 (2022) e202200513, https://doi.org/10.1002/celc.202200513.
[26] A. Gamero-Quijano, G. Herzog, P. Peljo, M.D. Scanlon, Electrocatalysis at the polarised interface between two immiscible electrolyte solutions, Curr. Opin. Electrochem. 38 (2023), 101212, https://doi.org/10.1016/j.coelec.2023.101212.
[27] T.J. Stockmann, Z. Ding, Hydrophobicity of room temperature ionic liquids assessed by the Galvani potential difference established at micro liquid/liquid interfaces, J. Electroanal. Chem. 649 (2010) 23–31, https://doi.org/10.1016/j.jelechem.2009.12.024.
[28] C. Batchelor-McAuley, C.A. Little, S.V. Sokolov, E. Katelhon, G. Zampardi, R. G. Compton, Fluorescence monitored voltammetry of single attoliter droplets, Anal. Chem. 88 (2016) 11213–11221, https://doi.org/10.1021/acs.analchem.6b03524.
[29] C.E. Banks, T.J. Davies, R.G. Evans, G. Hignett, A.J. Wain, N.S. Lawrence, J. D. Wadhawan, F. Marken, R.G. Compton, Electrochemistry of immobilised redox droplets: concepts and applications, Phys. Chem. Chem. Phys. 5 (2003) 4053–4069, https://doi.org/10.1039/B307326M.
[30] F. Scholz, U. Schroder, R. Gulaboski, A. Domenech-Carbo, Immobilized droplets, in Electrochemistry of Immobilized Particles and Droplets, Springer (2015) 225.
[31] S. Komorsky-Lovric, M. Lovric, F. Scholz, Cyclic voltammetry of decamethylferrocene at the organic liquid|aqueous solution|graphite three-phase junction, J. Electroanal. Chem. 508 (2001) 129–137, https://doi.org/10.1016/S0022-0728(01)00527-7.
[32] H. Deng, P. Peljo, T.J. Stockmann, L. Qiao, T. Vainikka, K. Kontturi, M. Opallo, H. H. Girault, Surprising acidity of hydrated lithium cations in organic solvents, Chem. Commun. 50 (2014) 5554–5557, https://doi.org/10.1039/C4CC01892C.
[33] S. Rastgar, K.T. Santos, C.A. Angelucci, G. Wittstock, Catalytic activity of alkali metal cations for the chemical oxygen reduction reaction in a biphasic liquid system probed by scanning electrochemical microscopy, Chem. Eur. J. 26 (2020) 10882–10890, https://doi.org/10.1002/chem.202001967.
[34] G. Shul, W. Adamiak, M. Opallo, Ion insertion into ionic liquid supported toluene generated by electrochemical redox reaction, Electrochem. Commun. 10 (2008) 1201–1204, https://doi.org/10.1016/j.elecom.2008.05.048.
[35] A.M. Bond, F. Marken, Mechanistic aspects of the electron and ion transport processes across the electrode|solid|solvent (electrolyte) interface of microcrystalline decamethylferrocene attached mechanically to a graphite electrode, J. Electroanal. Chem. 372 (1994) 125–135, https://doi.org/10.1016/0022-0728(93)03257-P.
[36] D. Wei, A. Ivaska, Applications of ionic liquids in electrochemical sensors, Anal. Chem. Acta 607 (2008) 126–135, https://doi.org/10.1016/j.aca.2007.12.011.
[37] M. Opallo, A. Lesniewski, A review on electrodes modified with ionic liquids, J. Electroanal. Chem. 656 (2011) 2–16, https://doi.org/10.1016/j.jelechem.2011.01.008.
[38] X. Wang, M. Salari, D. Jiang, J. Chapman Varela, B. Anasori, D.J. Wesolowski, S. Dai, M.W. Grinstaff, Y. Gogotsi, Electrode material–ionic liquid coupling for electrochemical energy storage, Nature Rev. Mater. 5 (2020) 787–808, https://doi.org/10.1038/s41578-020-0218-9.
[39] X. Liu, Z. Nan, Y. Qiu, L. Zheng, X. Lu, Hydrophobic ionic liquid immobilizing cholesterol oxidase on the electrodeposited Prussian blue on glassy carbon electrode for detection of cholesterol, Electrochim. Acta 90 (2013) 203–209, https://doi.org/10.1016/j.electacta.2012.11.119.
[40] J. Czarnecki, K.h. Khristov, J. Masliyah, N. Panchev, S.D. Taylor, P. Tchoukov, Application of Scheludko-Exerowa thin liquid film technique to studies of petroleum W/O emulsions, Coll. Surf. A 519 (2017) 2–10, https://doi.org/10.1016/j.colsurfa.2016.04.040.